

Optimal control theory for maximum output power of Brownian heat engines

Jin-Fu Chen^{1,*} and H. T. Quan^{1,2,3,†}

¹*School of Physics, Peking University, Beijing, 100871, China*

²*Collaborative Innovation Center of Quantum Matter, Beijing 100871, China*

³*Frontiers Science Center for Nano-optoelectronics, Peking University, Beijing, 100871, China*

(Dated: October 31, 2024)

The pursuit of achieving the maximum output power in microscopic heat engines has gained increasing attention in the field of stochastic thermodynamics. We employ the optimal control theory to study Brownian heat engines and determine the optimal heat-engine cycles in generic damped situation, which were previously known only in the overdamped and the underdamped limits. These optimal cycles include two isothermal processes, two adiabatic processes, and an extra isochoric relaxation process at the high stiffness constraint. Our results determine the maximum output power under realistic control constraints, and also bridge the gap of the optimal cycles between the overdamped and the underdamped limits. Hence, we solve an outstanding problem in the studies of heat engines by employing the optimal control theory to stochastic thermodynamics. These findings bring valuable insights for the design of high-performance Brownian heat engines in experimental setups.

Introduction. The output power is an important index to characterize the performance of real heat engines. To achieve efficient energy conversion at the nanoscale, Brownian heat engines were invented to extract useful work by harnessing the fluctuation and dissipation of a single Brownian particle [1–6]. The output power of these microscopic heat engines is significantly influenced by the coupling strength between the Brownian particle and the heat bath (characterized by the friction coefficient) and the control protocol of heat-engine cycles. However, what are the optimal friction coefficient and the optimal control protocol to achieve the maximum output power remain outstanding unsolved problems in the studies of heat engines. For Brownian heat engines, the previous optimization was limited to either the overdamped limit (large friction coefficient) [7–14] or the underdamped limit (small friction coefficient) [15, 16]. In the underdamped limit, the efficiency at the maximum output power agrees with Curzon and Ahborn’s prediction [17]. The output power diminishes in both the overdamped and the underdamped limits. It is expected that larger output power can be achieved with intermediate friction coefficient. Nevertheless, all the previous methods fail in this regime [15].

Recently, the thermodynamic geometry [18–23] has been applied to optimize control protocols of thermodynamic processes in the slow-driving regime [24–32]. However, these slow-driving protocols are not necessarily optimal to achieve the maximum output power since the optimal heat-engine cycles may operate far beyond the slow-driving regime. By contrast, a more elaborate optimization method is to employ the optimal control theory [33], which has been extensively employed in different subfields of physics, such as, optimal controls of closed and open quantum systems [34–39] and quantum

algorithms [40, 41]. The optimal control theory has also been employed to optimize ideal-gas heat-engine cycles in the framework of phenomenological finite-time thermodynamics [42–46]. Nevertheless, these models are based on the phenomenological assumption of Newton’s cooling law and lack the equation of motion. Hence, their results were still limited to the weak-coupling regime. Stochastic thermodynamics, on the other hand, is a framework of nonequilibrium thermodynamics characterizing irreversibility and fluctuations based on the equation of motion. It is valid for arbitrary friction coefficient, and it brings more insights such as fluctuation theorems [47, 48] and thermodynamic uncertainty relation [49, 50] than the phenomenological finite-time thermodynamics. However, the optimal control theory has not been applied to stochastic thermodynamics previously (see Ref. [51]).

In this Letter, we employ the optimal control theory to investigate the maximum output power of Brownian heat engines in the framework of stochastic thermodynamics. Our method of determining the optimal control protocol is valid for arbitrary friction coefficient. Under given control constraints of the stiffness and the bath temperature, we find a family of cycles with conserved pseudo-Hamiltonian, which is introduced by the Pontryagin maximum principle [33]. The optimal cycle is the one with the largest pseudo-Hamiltonian promising the maximum output power. Based on this microscopic model, we also bridge the gap of the optimal cycles between the overdamped [7, 8] and the underdamped limits [15, 16]. Thus, by employing the optimal control theory, we solve the outstanding problems of determining the optimal friction coefficient and the optimal control protocol to achieve the maximum output power of Brownian heat engines. Our results indicate that the most powerful heat engines operate at an intermediate friction coefficient, neither too small (underdamped limit) nor too large (overdamped limit). Our optimal cycles guide the design of Brownian heat engines in experimental setups [3, 52, 53].

* chenjinfu@pku.edu.cn

† htquan@pku.edu.cn

Setup and optimal isothermal processes. We consider a microscopic heat engine with a single Brownian particle as the working substance [1, 3, 8, 16]. The Hamiltonian of the system is

$$H = \frac{p^2}{2} + \frac{1}{2}\lambda x^2, \quad (1)$$

where the mass of the particle is set unity, and the work parameter λ is the stiffness of the harmonic potential. The system is coupled to a heat bath at temperature T_b . The stiffness λ and the bath temperature T_b can be varied by an external agent to construct heat-engine cycles. The evolution of the distribution $\rho(x, p, t)$ of position and momentum is described by the Fokker-Planck equation [54]

$$\frac{\partial \rho}{\partial t} = -\frac{\partial}{\partial x}(p\rho) + \frac{\partial}{\partial p}(\lambda x\rho + \kappa p\rho + \kappa T_b \frac{\partial \rho}{\partial p}), \quad (2)$$

with the friction coefficient κ . The distribution remains Gaussian during the evolution when the system evolves from an initial Gaussian state. We characterize the state of the system with the covariances of position and momentum $\Gamma = (\Gamma_{xx}, \Gamma_{xp}, \Gamma_{pp})^T$ with $\Gamma_{xx} = \langle x^2 \rangle$, $\Gamma_{xp} = \langle xp \rangle$, and $\Gamma_{pp} = \langle p^2 \rangle$, satisfying [55, 56]

$$\dot{\Gamma} = L\Gamma + f, \quad (3)$$

$$L = \begin{pmatrix} 0 & 2 & 0 \\ -\lambda & -\kappa & 1 \\ 0 & -2\lambda & -2\kappa \end{pmatrix}, \quad (4)$$

with $f = (0, 0, 2\kappa T_b)^T$. The real parts of L 's eigenvalues $l_1 = -\kappa + \sqrt{\kappa^2 - 4\lambda}$, $l_2 = -\kappa$, and $l_3 = -\kappa - \sqrt{\kappa^2 - 4\lambda}$ determine the relaxation rates of covariances. The relaxation rate of position is determined by the minimal real part of these eigenvalues, i.e., $\Delta = -\text{Re}(l_1)$. The work performed on the system is $\dot{W} = \dot{\lambda}\Gamma_{xx}/2$. By substituting $\Gamma_{xp} = \dot{\Gamma}_{xx}/2$ and $\Gamma_{pp} = (\kappa\dot{\Gamma}_{xx} + 2\lambda\Gamma_{xx} + \dot{\Gamma}_{xx})/2$ into Eq. (3), we obtain a high-order differential equation of Γ_{xx} as

$$\ddot{\Gamma}_{xx} + 3\kappa\dot{\Gamma}_{xx} + (2\kappa^2 + 4\lambda)\dot{\Gamma}_{xx} = 4\kappa T_b - (2\dot{\lambda} + 4\kappa\lambda)\Gamma_{xx}. \quad (5)$$

It is challenging to solve the optimal control problem of minimizing the performed work based on the exact equation (3) of motion [or Eq. (5)], since the system is not fully controllable [33]: there are three state variables Γ_{xx} , Γ_{xp} and Γ_{pp} but only two parameters λ and T_b can be varied.

To simplify the optimal control problem, we focus on relatively slow control $\dot{\lambda}/\lambda < \Delta$ with slowly varying $\dot{\Gamma}_{xx}$ such that the higher-order derivatives in Eq. (5) can be neglected. Such approximation renders the system controllable [33], and Eq. (5) is simplified into

$$\dot{\Gamma}_{xx} = -\frac{2\kappa\lambda}{\kappa^2 + 2\lambda}\left(\Gamma_{xx} - \frac{T_b}{\lambda}\right) - \frac{\dot{\lambda}}{\kappa^2 + 2\lambda}\Gamma_{xx}, \quad (6)$$

which is rewritten in the form of the potential energy $V \equiv \lambda\Gamma_{xx}/2$ as

$$\dot{V} = \frac{(\kappa^2 + \lambda)\dot{\lambda}}{(\kappa^2 + 2\lambda)\lambda}V - \frac{\kappa\lambda(2V - T_b)}{(\kappa^2 + 2\lambda)}. \quad (7)$$

We will use the approximate equation (7) of motion to solve the optimal control protocol of varying $\lambda(t)$, and propagate the exact equation (3) of motion with the solved protocol. The optimal cycles, constructed by the optimal control protocols and the switchings, indeed leads to large output power for the intermediate friction coefficient, where the previous protocols of heat-engine cycles [7, 8, 15, 16] in the underdamped and overdamped limits fail. We will validate the approximate equation (6) of motion with different friction coefficients in the domain of its applicability $\dot{\lambda}/\lambda < \Delta$.

We now employ the optimal control theory to the control of the stiffness and the bath temperature. The potential energy V and the stiffness λ are state variables in the control problem. The control parameters are the rate of stiffness change $\alpha = \dot{\lambda}/\lambda$ and the bath temperature T_b . The control constraints are $\lambda_L \leq \lambda \leq \lambda_H$ and $T_L \leq T_b \leq T_H$. The output work of a cycle is $W_{\text{out}} = -\int_0^T \alpha V dt$, and is the goal of the optimization. The pseudo-Hamiltonian of the optimal control theory for this system is constructed as [57]

$$\mathcal{H} = -\alpha V + \psi_V \frac{(\kappa^2 + \lambda)\alpha V - \kappa\lambda(2V - T_b)}{\kappa^2 + 2\lambda} + \psi_\lambda \alpha \lambda, \quad (8)$$

where ψ_V and ψ_λ are costate variables [33, 42]. The pseudo-Hamiltonian \mathcal{H} is introduced to derive the optimal control protocol, and should be distinguished from the Hamiltonian H of the system. The evolution of the state variables is governed by $\dot{V} = \partial\mathcal{H}/\partial\psi_V$ [Eq. (7)] and $\dot{\lambda} = \partial\mathcal{H}/\partial\psi_\lambda = \alpha\lambda$, while the evolution of the costate variables is governed by

$$\dot{\psi}_V = -\frac{\partial\mathcal{H}}{\partial V} = \alpha - \psi_V \frac{\alpha(\kappa^2 + \lambda) - 2\kappa\lambda}{\kappa^2 + 2\lambda}, \quad (9)$$

$$\dot{\psi}_\lambda = -\frac{\partial\mathcal{H}}{\partial\lambda} = \psi_V \frac{\kappa^2(V(\alpha + 2\kappa) - \kappa T_b)}{(\kappa^2 + 2\lambda)^2} - \alpha\psi_\lambda. \quad (10)$$

The control parameters α and T_b are chosen to maximize \mathcal{H} under the control constraints. The control protocol of the bath temperature T_b is determined by

$$\frac{\partial\mathcal{H}}{\partial T_b} = \frac{\kappa\lambda\psi_V}{\kappa^2 + 2\lambda}, \quad (11)$$

which corresponds to a bang-bang control $T_b = T_H$ for $\psi_V > 0$ and $T_b = T_L$ for $\psi_V < 0$. The control protocol of the stiffness change rate α is determined by

$$\frac{\partial\mathcal{H}}{\partial\alpha} = \lambda\psi_\lambda + \frac{V(\kappa^2 + \lambda)\psi_V}{\kappa^2 + 2\lambda} - V. \quad (12)$$

Due to the fact that the right hand side of Eq. (12) does not depend on α , we first consider the singular control with $\partial\mathcal{H}/\partial\alpha = 0$ [33]. The costate variables and the rate of stiffness change are solved as

$$\psi_V = \frac{(\kappa^2 + 2\lambda)(T_b - 2V)}{\lambda T_b + 2\kappa^2 V}, \quad (13)$$

$$\psi_\lambda = \frac{V[2V(2\kappa^2 + \lambda) - \kappa^2 T_b]}{\lambda(\lambda T_b + 2\kappa^2 V)}, \quad (14)$$

$$\frac{\dot{\lambda}}{\lambda} = \frac{\kappa\lambda(2V - T_b)[2\kappa^2 V + (\kappa^2 + 2\lambda)T_b]}{V[4\kappa^4 V + 6\kappa^2\lambda V + (\kappa^2 + 2\lambda)\lambda T_b]}, \quad (15)$$

where Eq. (15) gives the optimal control protocols of isothermal processes.

We eliminate the costate variables with Eqs. (13) and (14), and obtain the pseudo-Hamiltonian

$$\mathcal{H} = \frac{\kappa\lambda(T_b - 2V)^2}{\lambda T_b + 2\kappa^2 V}, \quad (16)$$

whose magnitude encodes the information of the velocity of the control. In quasistatic isothermal processes, the system is in equilibrium with the heat bath, i.e., $V = T_b/2$, and thus $\mathcal{H} = 0$. In nonquasistatic isothermal processes, we can solve V of the optimal control from the conservation of \mathcal{H} as

$$V = \frac{T_b}{2} + \frac{\kappa\mathcal{H}}{4\lambda} \left[1 - \epsilon \sqrt{1 + \frac{4\lambda T_b}{\kappa\mathcal{H}} \left(1 + \frac{\lambda}{\kappa^2} \right)} \right], \quad (17)$$

where $\epsilon = +1$ for the expansion process and -1 for the compression process.

The control protocol can be significantly simplified in the two limits. In the overdamped limit $\kappa^2 \gg \lambda$, the pseudo-Hamiltonian Eq. (16) becomes $\mathcal{H} = \lambda(T_b - 2V)^2/(2\kappa V)$, and the control protocol of the stiffness and the evolution of the potential energy are

$$\lambda(t) = \frac{\lambda_0[1 - \mathcal{H}t/(2V_0)]}{\left(1 + \epsilon \sqrt{\lambda_0\mathcal{H}/(2\kappa V_0)}t \right)^2}, \quad (18)$$

$$V(t) = V_0 - \mathcal{H}t/2. \quad (19)$$

The above protocol agrees with that obtained in Ref. [7]. In the underdamped limit $\kappa^2 \ll \lambda$, the pseudo-Hamiltonian Eq. (16) becomes $\mathcal{H} = \kappa(T_b - 2V)^2/T_b$. The potential energy V of the optimal control thus remains constant in nonquasistatic isothermal processes

$$V(t) = \frac{T_b}{2} - \frac{\epsilon}{2} \sqrt{\frac{\mathcal{H}T_b}{\kappa}}, \quad (20)$$

and the control protocol is the exponential protocol

$$\frac{\dot{\lambda}}{\lambda} = \frac{2\kappa}{1 - \epsilon \sqrt{\kappa T_b/\mathcal{H}}} = \text{const}, \quad (21)$$

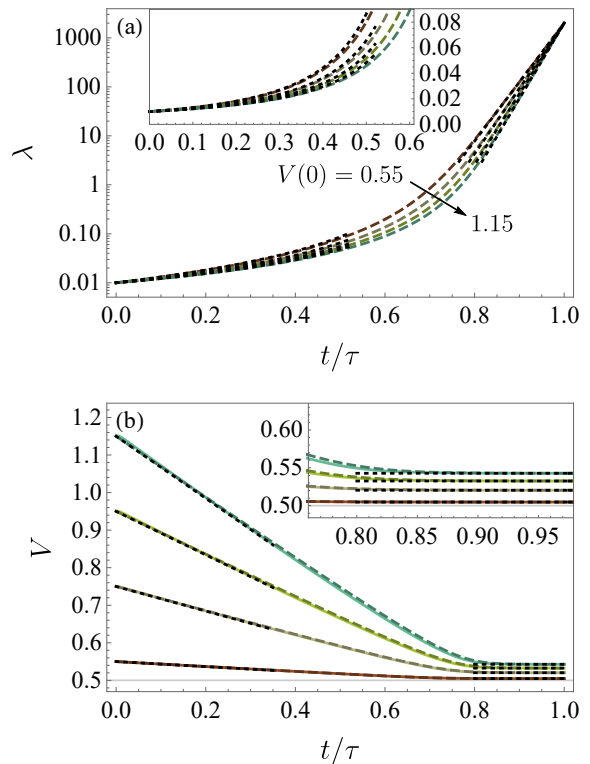


Figure 1. The optimal control of isothermal processes in the generic damped situation (arbitrary friction coefficient). The parameters are set as $T_b = 1$ and $\kappa = 1$. (a) The optimal control protocols with different control speeds characterized by $V(0) = 0.55, 0.75, 0.95,$ and 1.15 . We plot all the protocols (dashed curves) with a rescaled time t/τ and the initial and final stiffness $\lambda(0) = 0.01$ and $\lambda(\tau) = 2000$. (b) The evolution of the potential energy V during the isothermal processes. The solid curves show the results of the exact equation (3) of motion with the protocols in Fig. 1(a). In both subfigures, the dotted lines show the results in the overdamped and the underdamped limits, and the dashed curves represent the approximate results obtained from Eqs. (7) and (15).

which agrees with that obtained in Refs. [58, 59].

It is desirable to check the validity of the approximation used in Eq. (6). After solving the protocols from Eqs. (7) and (15), we can utilize these protocols to propagate the exact equation (3) of motion. Figure 1(a) shows the control protocols of the stiffness $\lambda(t)$ (dashed curves) with a rescaled time t/τ for the isothermal compression processes. The black dotted curves represent the optimal control protocols in the overdamped limit [7, 8] and the underdamped limit [15, 16], agreeing with our protocols at the initial and final stages, respectively. The results of the evolution of potential energy are compared in Fig. 1(b). We set the bath temperature $T_b = 1$, the friction coefficient $\kappa = 1$, and the initial and final stiffness $\lambda(0) = 0.01$ and $\lambda(\tau) = 2000$, and choose the initial potential energy as $V(0) = 0.55, 0.75, 0.95,$ and 1.15 . With larger $V(0)$, the isothermal compression is

carried out more rapidly. The dashed curves are solved based on the approximate equation (7) of motion, while the solid curves show the exact evolution by propagating Eq. (3) with the protocols in Fig. 1(a). The agreement of the solid curves and the dashed curves validates the approximation used in Eq. (6), at least in the domain of its applicability.

Construction of the optimal cycles. We continue to construct heat-engine cycles under the control constraints $\lambda_L \leq \lambda \leq \lambda_H$ and $T_L \leq T_b \leq T_H$. During the whole cycle, the pseudo-Hamiltonian is conserved and we thus require two isothermal processes with identical \mathcal{H} . For a given \mathcal{H} , we find two switchings at the stiffness constraints λ_L and λ_H are necessary: T_b and λ are changed simultaneously and instantaneously [57]. Thus, \mathcal{H} together with the control constraints determines the control protocol of the cycle.

During the switchings, both λ and T_b are changed instantaneously, i.e., $\alpha \gg \kappa$, and the evolution equations (7) and (9) are reduced to

$$\dot{V} = \frac{\kappa^2 + \lambda}{\kappa^2 + 2\lambda} \alpha V, \quad (22)$$

$$\dot{\psi}_V = \alpha \left[1 - \frac{(\kappa^2 + \lambda)}{\kappa^2 + 2\lambda} \psi_V \right]. \quad (23)$$

The initial and final values during the switchings satisfy

$$\frac{V_f \sqrt{\kappa^2 + 2\lambda_f}}{\lambda_i} = \frac{V_i \sqrt{2\lambda_i + \kappa^2}}{\lambda_i}, \quad (24)$$

$$\frac{\lambda_f (\psi_{Vf} - 2) - \kappa^2}{\sqrt{\kappa^2 + 2\lambda_f}} = \frac{\lambda_i (\psi_{Vi} - 2) - \kappa^2}{\sqrt{\kappa^2 + 2\lambda_i}}. \quad (25)$$

The two switchings II and V in a cycle are given by $\lambda_2 \rightarrow \lambda_H, V_2 \rightarrow V_3, \psi_{V2} \rightarrow \psi_{V3}$ and $\lambda_5 \rightarrow \lambda_L, V_5 \rightarrow V_6, \psi_{V5} \rightarrow \psi_{V6}$, as shown in Fig. 2(a). The six boundary points and the six processes are denoted as 1, 2, ..., 6 and I, II, ..., VI, respectively. The two switchings are solved from the conservation of \mathcal{H} [57]. By increasing \mathcal{H} , point 6 will approach point 1 on the cold isothermal curve. Since larger \mathcal{H} leads to larger output power, we consider the maximum \mathcal{H} such that the cycle still reaches λ_L . The output power P of the maximum- \mathcal{H} cycle is evaluated as

$$P = - \frac{W_I + W_{II} + W_{IV} + W_V}{\tau_I + \tau_{III} + \tau_{IV}}. \quad (26)$$

The expressions of the work and the operation time of each process are given in [57].

With the above protocol of a whole cycle, we can propagate the exact equation (3) of motion and obtain the exact output power of the limit cycle. In accordance with Eq. (26), we choose the connecting processes to be thermodynamic adiabatic (unitary) processes that satisfy $\Gamma_{pp}^f \Gamma_{xx}^f = \Gamma_{pp}^i \Gamma_{xx}^i$. In principle, such unitary evolution can be carried out in arbitrarily short time by choosing a large Hamiltonian [60, 61]. The corresponding protocol

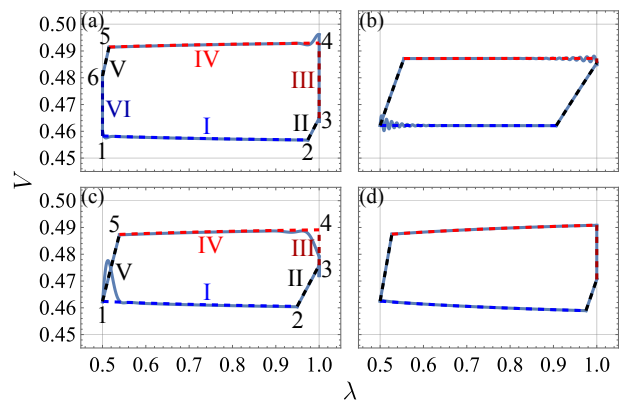


Figure 2. Diagrams of Brownian heat-engine cycles. (a) $\kappa = 1$ and $\mathcal{H} = 10^{-4}$ (nonmaximum \mathcal{H}), (b) $\kappa = 0.1$ (underdamped, maximum \mathcal{H}), (c) $\kappa = 0.83$ (optimal, maximum \mathcal{H}), and (d) $\kappa = 10$ (overdamped, maximum \mathcal{H}). The control constraints are $T_L = 0.9, T_H = 1, \lambda_L = 0.5$ and $\lambda_H = 1$. The solid and the dashed curves represent limit cycles according to the exact equation (3) and the approximate equation (7) of motion, respectively.

to vary the Hamiltonian can be realized by adopting the shortcut to adiabaticity [62, 63]. After solving Γ_{xx}, Γ_{xp} , and Γ_{pp} during the exact evolution of the whole cycle, we use Eq. (26) to evaluate the exact output power.

We plot diagrams of heat-engine cycles in Fig. 2 for a non-maximum- \mathcal{H} cycle with (a) $\kappa = 1$ and $\mathcal{H} = 10^{-4}$, and three maximum- \mathcal{H} cycles with (b) $\kappa = 0.1$ (underdamped), (c) $\kappa = 0.83$ (optimal), and (d) $\kappa = 10$ (overdamped). In the underdamped limit [Fig. 2(b)], the optimal protocol of the cycle recovers that of the Curzon-Ahlborn engine [16, 17], and the effective temperature of the Brownian particle remains constant ($V = \text{const}$) during the isothermal processes. For an intermediate friction coefficient [Fig. 2(c)], the exact evolution (solid curves) deviates slightly from the approximate evolution (dashed curves), and the exact output power is similar to the approximate output power. In the overdamped limit [Fig. 2(d)], the protocols of the two isothermal processes recover those in Refs. [7, 8].

Maximum output power of Brownian heat engines. For a given friction coefficient κ , we evaluate the output power P of maximum- \mathcal{H} cycles. Furthermore, the friction coefficient κ can be adjusted to achieve the maximum output power. In a generic damped situation (arbitrary friction coefficient), we solve the maximum- \mathcal{H} cycle numerically. Analytical results are obtained in the overdamped limit and the underdamped limit.

In the overdamped limit $\kappa^2 \gg \lambda_H$, the cooling rate according to Eq. (7) is equal to $2\lambda/\kappa$. Thus, the output power is inversely proportional to the friction coefficient $P_{\text{over}} \propto 1/\kappa$ [57]. We can choose λ_L as large as possible so that the maximum output power P_{over}^* can be achieved by the sliced cycles [57]

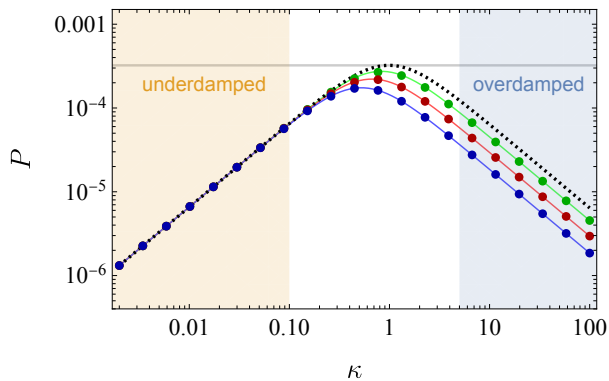


Figure 3. Output power of the optimal cycles for different friction coefficients. We set the control constraints $T_L = 0.9$, $T_H = 1$, $\lambda_H = 1$, and choose different $\lambda_L = 1/8$ (blue), $1/4$ (red), $1/2$ (green). The dots and the solid curves show the results of the exact evolution [Eq. (3)] and the approximate evolution [Eq. (7)], respectively. The black dotted curve shows the maximum output power of sliced cycles, and the gray horizontal line shows the maximum output power.

$$P_{\text{over}}^* = \frac{\lambda_H T_H}{\kappa} \phi\left(\frac{T_L}{T_H}\right), \quad (27)$$

where $\phi(\theta)$ is the positive root of the polynomial

$$\phi^3 + (11 - 3\theta)\phi^2 + (3\theta^2 + 14\theta - 1)\phi - (\theta - 1)^2\theta = 0, \quad (28)$$

with $\theta = T_L/T_H$. A detailed discussion of these sliced cycles is left in [57].

In the underdamped limit $\kappa^2 \ll \lambda_L$, the maximum output power is [15, 16]

$$P_{\text{under}}^* = \frac{\kappa T_H}{4} \left(1 - \sqrt{\frac{T_L}{T_H}}\right)^2. \quad (29)$$

We left the derivations of Eqs. (27) and (29) in [57]. This maximum output power also agrees with the results of ideal-gas heat engines based on Newton's cooling law [42, 43].

Figure 3 illustrates the output power P of maximum- \mathcal{H} cycles as a function of the friction coefficient κ . We set the control constraints $T_H = 1$, $T_L = 0.9$, $\lambda_H = 1$, and choose different $\lambda_L = 1/8$ (blue), $1/4$ (red), $1/2$

(green). The output power of the exact evolution (dots) agrees well with that of the approximate evolution (solid curves), and is bounded by the maximum output power of sliced cycles (black dotted curve) [57]. The maximum output power in the generic damped situation also recovers that in both the overdamped and the underdamped limits. The gray horizontal line shows the maximum output power [57]. The maximum power can be achieved at the intermediate friction coefficient. This fact can be explained by the relaxation rate of position $\Delta = \text{Re}(\kappa - \sqrt{\kappa^2 - 4\lambda})$. Rapid relaxation of position is achieved for large Δ , which corresponds to $\kappa \sim 2\sqrt{\lambda}$.

Conclusion. The maximum output power of Brownian heat engines in the overdamped and the underdamped limits has been obtained previously [7, 8, 15, 16], but what are the maximum output power and the corresponding optimal control protocol in generic damped situation (for an arbitrary friction coefficient) are outstanding unsolved problems in the studies of heat engines. Previous methods fail [15] in this situation due to the lack of timescale separation.

In this work, we employ the optimal control theory to stochastic thermodynamics, and solve the outstanding problem of determining the optimal friction coefficient and the optimal control protocol to achieve the maximum output power of Brownian heat engines. We construct the optimal cycles in generic damped situation based on the approximate equation of motion. These optimal cycles include two isothermal processes, two adiabatic processes, and an extra isochoric relaxation process at the high stiffness constraint. It is found that powerful heat engines correspond to the intermediate friction coefficient, neither too small (underdamped limit) nor too large (overdamped limit). This argument should also be valid for quantum heat engines [64–66].

Our findings show the effectiveness of the optimal control theory in stochastic thermodynamics, and provide practical guidance for the experimental design of Brownian heat engines. It is interesting to explore the trade-off relation between efficiency and output power of Brownian heat engines in generic damped situation and also the optimal control protocol of cycles to achieve the maximum output power at a given efficiency [67–71], and we leave these problems for future investigation.

Acknowledgment. This work is supported by the National Natural Science Foundation of China (NSFC) under Grants No. 12147157, No. 11775001, No. 11825501, and No. 12375028.

-
- [1] V. Blickle and C. Bechinger, Realization of a micrometre-sized stochastic heat engine, *Nat. Phys.* **8**, 143 (2012).
 [2] P. A. Quinto-Su, A microscopic steam engine implemented in an optical tweezer, *Nat. Commun.* **5**, 5889 (2014).
 [3] I. A. Martínez, É. Roldán, L. Dinis, D. Petrov, J. M. R.

- Parrondo, and R. A. Rica, Brownian Carnot engine, *Nat. Phys.* **12**, 67 (2016).
 [4] S. Krishnamurthy, S. Ghosh, D. Chatterji, R. Ganapathy, and A. K. Sood, A micrometre-sized heat engine operating between bacterial reservoirs, *Nat. Phys.* **12**, 1134 (2016).

- [5] I. A. Martínez, É. Roldán, L. Dinis, and R. A. Rica, Colloidal heat engines: a review, *Soft Matter* **13**, 22 (2017).
- [6] V. Holubec and A. Ryabov, Fluctuations in heat engines, *J. Phys. A: Math. Theor.* **55**, 013001 (2021).
- [7] T. Schmiedl and U. Seifert, Optimal finite-time processes in stochastic thermodynamics, *Phys. Rev. Lett.* **98**, 108301 (2007).
- [8] T. Schmiedl and U. Seifert, Efficiency at maximum power: An analytically solvable model for stochastic heat engines, *Europhys. Lett.* **81**, 20003 (2007).
- [9] P. R. Zulkowski and M. R. DeWeese, Optimal control of overdamped systems, *Phys. Rev. E* **92**, 032117 (2015).
- [10] C. A. Plata, D. Guéry-Odelin, E. Trizac, and A. Prados, Optimal work in a harmonic trap with bounded stiffness, *Phys. Rev. E* **99**, 012140 (2019).
- [11] K. Proesmans, J. Ehrich, and J. Bechhoefer, Finite-Time Landauer Principle, *Phys. Rev. Lett.* **125**, 100602 (2020).
- [12] Z. Ye, F. Cerisola, P. Abiuso, J. Anders, M. Perarnau-Llobet, and V. Holubec, Optimal finite-time heat engines under constrained control, *Phys. Rev. Research* **4**, 043130 (2022).
- [13] G.-H. Xu, C. Jiang, Y. Minami, and G. Watanabe, Relation between fluctuations and efficiency at maximum power for small heat engines, *Phys. Rev. Research* **4**, 043139 (2022).
- [14] P. Abiuso, V. Holubec, J. Anders, Z. Ye, F. Cerisola, and M. Perarnau-Llobet, Thermodynamics and optimal protocols of multidimensional quadratic Brownian systems, *J. Phys. Commun.* **6**, 063001 (2022).
- [15] A. Dechant, N. Kiesel, and E. Lutz, Underdamped stochastic heat engine at maximum efficiency, *Europhys. Lett.* **119**, 50003 (2017).
- [16] Y. H. Chen, J.-F. Chen, Z. Fei, and H. T. Quan, Microscopic theory of the Curzon-Ahlborn heat engine based on a Brownian particle, *Phys. Rev. E* **106**, 024105 (2022).
- [17] F. L. Curzon and B. Ahlborn, Efficiency of a Carnot engine at maximum power output, *Am. J. Phys* **43**, 22 (1975).
- [18] P. Salamon and R. S. Berry, Thermodynamic Length and Dissipated Availability, *Phys. Rev. Lett.* **51**, 1127 (1983).
- [19] G. E. Crooks, Measuring Thermodynamic Length, *Phys. Rev. Lett.* **99**, 100602 (2007).
- [20] D. A. Sivak and G. E. Crooks, Thermodynamic Metrics and Optimal Paths, *Phys. Rev. Lett.* **108**, 190602 (2012).
- [21] P. R. Zulkowski, D. A. Sivak, G. E. Crooks, and M. R. DeWeese, Geometry of thermodynamic control, *Phys. Rev. E* **86**, 041148 (2012).
- [22] M. Scandi and M. Perarnau-Llobet, Thermodynamic length in open quantum systems, *Quantum* **3**, 197 (2019).
- [23] S. Blaber and D. A. Sivak, Optimal control in stochastic thermodynamics, *J. Phys. Commun.* **7**, 033001 (2023).
- [24] V. Cavina, A. Mari, and V. Giovannetti, Slow Dynamics and Thermodynamics of Open Quantum Systems, *Phys. Rev. Lett.* **119**, 050601 (2017).
- [25] K. Brandner and K. Saito, Thermodynamic Geometry of Microscopic Heat Engines, *Phys. Rev. Lett.* **124**, 040602 (2020).
- [26] J.-F. Chen, C. P. Sun, and H. Dong, Extrapolating the thermodynamic length with finite-time measurements, *Phys. Rev. E* **104**, 034117 (2021).
- [27] P. Abiuso and M. Perarnau-Llobet, Optimal Cycles for Low-Dissipation Heat Engines, *Phys. Rev. Lett.* **124**, 110606 (2020).
- [28] G. Li, J.-F. Chen, C. P. Sun, and H. Dong, Geodesic Path for the Minimal Energy Cost in Shortcuts to Isothermality, *Phys. Rev. Lett.* **128**, 230603 (2022).
- [29] J.-F. Chen, Optimizing Brownian heat engine with shortcut strategy, *Phys. Rev. E* **106**, 054108 (2022).
- [30] A. G. Frim and M. R. DeWeese, Geometric Bound on the Efficiency of Irreversible Thermodynamic Cycles, *Phys. Rev. Lett.* **128**, 230601 (2022).
- [31] Z. Wang and J. Ren, Thermodynamic Geometry of Nonequilibrium Fluctuations in Cyclically Driven Transport, (2023), 10.48550/ARXIV.2304.08181, arXiv:2304.08181 [cond-mat.stat-mech].
- [32] J.-F. Chen, R.-X. Zhai, C. P. Sun, and H. Dong, Geodesic Lower Bound of the Energy Consumption to Achieve Membrane Separation within Finite Time, *PRX Energy* **2**, 033003 (2023).
- [33] L. S. Pontryagin, V. G. Boltyanskii, R. V. Gamkrelidze, and E. F. Mishechenko, *The Mathematical Theory of Optimal Processes* (Wiley, New York, 1962).
- [34] A. P. Peirce, M. A. Dahleh, and H. Rabitz, Optimal control of quantum-mechanical systems: Existence, numerical approximation, and applications, *Phys. Rev. A* **37**, 4950 (1988).
- [35] T. Caneva, M. Murphy, T. Calarco, R. Fazio, S. Montangero, V. Giovannetti, and G. E. Santoro, Optimal Control at the Quantum Speed Limit, *Phys. Rev. Lett.* **103**, 240501 (2009).
- [36] S. Lloyd and S. Montangero, Information Theoretical Analysis of Quantum Optimal Control, *Phys. Rev. Lett.* **113**, 010502 (2014).
- [37] J. Li, X. Yang, X. Peng, and C.-P. Sun, Hybrid Quantum-Classical Approach to Quantum Optimal Control, *Phys. Rev. Lett.* **118**, 150503 (2017).
- [38] V. Cavina, A. Mari, A. Carlini, and V. Giovannetti, Optimal thermodynamic control in open quantum systems, *Phys. Rev. A* **98**, 012139 (2018).
- [39] U. Boscain, M. Sigalotti, and D. Sugny, Introduction to the Pontryagin Maximum Principle for Quantum Optimal Control, *PRX Quantum* **2**, 030203 (2021).
- [40] Z.-C. Yang, A. Rahmani, A. Shabani, H. Neven, and C. Chamon, Optimizing Variational Quantum Algorithms Using Pontryagin's Minimum Principle, *Phys. Rev. X* **7**, 021027 (2017).
- [41] L. T. Brady, C. L. Baldwin, A. Bapat, Y. Kharkov, and A. V. Gorshkov, Optimal Protocols in Quantum Annealing and Quantum Approximate Optimization Algorithm Problems, *Phys. Rev. Lett.* **126**, 070505 (2021).
- [42] M. H. Rubin, Optimal configuration of a class of irreversible heat engines. II, *Phys. Rev. A* **19**, 1277 (1979).
- [43] M. H. Rubin, Optimal configuration of an irreversible heat engine with fixed compression ratio, *Phys. Rev. A* **22**, 1741 (1980).
- [44] M. Mozurkewich and R. S. Berry, Optimal paths for thermodynamic systems: The ideal Otto cycle, *J. Appl. Phys.* **53**, 34 (1982).
- [45] B. Andresen, P. Salamon, and R. S. Berry, Thermodynamics in finite time, *Phys. Today* **37**, 62 (1984).
- [46] K. H. Hoffmann, S. J. Watowich, and R. S. Berry, Optimal paths for thermodynamic systems: The ideal diesel cycle, *J. Appl. Phys.* **58**, 2125 (1985).
- [47] C. Jarzynski, Nonequilibrium Equality for Free Energy Differences, *Phys. Rev. Lett.* **78**, 2690 (1997).
- [48] U. Seifert, Stochastic thermodynamics, fluctuation theorems and molecular machines, *Rep. Prog. Phys.* **75**, 126001 (2012).

- [49] A. C. Barato and U. Seifert, Thermodynamic uncertainty relation for biomolecular processes, *Phys. Rev. Lett.* **114**, 158101 (2015).
- [50] J. M. Horowitz and T. R. Gingrich, Proof of the finite-time thermodynamic uncertainty relation for steady-state currents, *Phys. Rev. E* **96**, 020103(R) (2017).
- [51] P. Muratore-Ginanneschi and K. Schwieger, How nanomechanical systems can minimize dissipation, *Phys. Rev. E* **90**, 060102(R) (2014).
- [52] T. M. Hoang, R. Pan, J. Ahn, J. Bang, H. T. Quan, and T. Li, Experimental Test of the Differential Fluctuation Theorem and a Generalized Jarzynski Equality for Arbitrary Initial States, *Phys. Rev. Lett.* **120**, 080602 (2018).
- [53] B. R. Ferrer, J. R. Gomez-Solano, and A. V. Arzola, Fluid Viscoelasticity Triggers Fast Transitions of a Brownian Particle in a Double Well Optical Potential, *Phys. Rev. Lett.* **126**, 108001 (2021).
- [54] H. Kramers, Brownian motion in a field of force and the diffusion model of chemical reactions, *Physica* **7**, 284 (1940).
- [55] Y. Rezek and R. Kosloff, Irreversible performance of a quantum harmonic heat engine, *New J. Phys.* **8**, 83 (2006).
- [56] J.-F. Chen and H. T. Quan, Hierarchical structure of fluctuation theorems for a driven system in contact with multiple heat reservoirs, *Phys. Rev. E* **107**, 024135 (2023).
- [57] Supplementary Materials, SupplementaryMaterials.
- [58] Z. Gong, Y. Lan, and H. T. Quan, Stochastic Thermodynamics of a Particle in a Box, *Phys. Rev. Lett.* **117**, 180603 (2016).
- [59] D. S. P. Salazar, Work distribution in thermal processes, *Phys. Rev. E* **101**, 030101(R) (2020).
- [60] L. Mandelstam and I. G. Tamm, The uncertainty relation between energy and time in nonrelativistic quantum mechanics, *J. Phys. USSR* **9**, 249 (1945).
- [61] N. Margolus and L. B. Levitin, The maximum speed of dynamical evolution, *Phys. D: Nonlinear Phenom.* **120**, 188 (1998).
- [62] M. V. Berry, Transitionless quantum driving, *J. Phys. A: Math. Theor.* **42**, 365303 (2009).
- [63] D. Guéry-Odelin, A. Ruschhaupt, A. Kiely, E. Torrontegui, S. Martínez-Garaot, and J. G. Muga, Shortcuts to adiabaticity: Concepts, methods, and applications, *Rev. Mod. Phys.* **91**, 045001 (2019).
- [64] R. Uzdin, A. Levy, and R. Kosloff, Quantum Heat Machines Equivalence, Work Extraction beyond Markovianity, and Strong Coupling via Heat Exchangers, *Entropy* **18**, 124 (2016).
- [65] D. Gelbwaser-Klimovsky and A. Aspuru-Guzik, Strongly Coupled Quantum Heat Machines, *J. Phys. Chem. Lett.* **6**, 3477 (2015).
- [66] M. Perarnau-Llobet, H. Wilming, A. Riera, R. Gallego, and J. Eisert, Strong Coupling Corrections in Quantum Thermodynamics, *Phys. Rev. Lett.* **120**, 120602 (2018).
- [67] L. Chen and Z. Yan, The effect of heat-transfer law on performance of a two-heat-source endoreversible cycle, *J. Chem. Phys.* **90**, 3740 (1989).
- [68] N. Shiraishi, K. Saito, and H. Tasaki, Universal trade-off relation between power and efficiency for heat engines, *Phys. Rev. Lett.* **117**, 190601 (2016).
- [69] V. Holubec and A. Ryabov, Maximum efficiency of low-dissipation heat engines at arbitrary power, *J. Stat. Mech: Theory Exp.* **2016**, 073204 (2016).
- [70] P. Pietzonka and U. Seifert, Universal trade-off between power, efficiency, and constancy in steady-state heat engines, *Phys. Rev. Lett.* **120**, 190602 (2018).
- [71] Y.-H. Ma, D. Xu, H. Dong, and C.-P. Sun, Universal constraint for efficiency and power of a low-dissipation heat engine, *Phys. Rev. E* **98**, 042112 (2018).

Supplementary materials: Optimal control theory for maximum power of Brownian heat engines

Jin-Fu Chen^{1,*} and H. T. Quan^{1,2,3,†}

¹*School of Physics, Peking University, Beijing, 100871, China*

²*Collaborative Innovation Center of Quantum Matter, Beijing 100871, China*

³*Frontiers Science Center for Nano-optoelectronics, Peking University, Beijing, 100871, China*

(Dated: October 31, 2024)

The supplementary materials are devoted to providing detailed derivations in the main context. In Sec. I, we show the derivations to the optimal control (Eqs. (13)-(17) in the main text) and the construction of the heat-engine cycles (Fig. 2 of the main text) based on the Pontryagin maximum principle for a Brownian heat engine in generic damped situation. The derivations in the underdamped and the overdamped limits are left in Sec. II and Sec. III, respectively. In Sec. IV, we discuss the results for the sliced cycles, which theoretically lead to the bound on the maximum power, i.e., the black dotted curve in Fig. 3 of the main text.

CONTENTS

I. Optimization in generic damped situation	1
A. Isothermal processes	2
B. Switchings: connecting processes	4
C. Construction of heat engine cycles	5
II. Optimization in underdamped limit	6
Construction of heat-engine cycles	7
III. Optimization in overdamped limit	9
Construction of heat-engine cycles	11
IV. Output power of sliced cycle	14
A. Generic damped situation	14
B. Overdamped limit	16
C. Underdamped limit	16
D. Maximum output power in generic damped situation	17
References	17

I. OPTIMIZATION IN GENERIC DAMPED SITUATION

We hope to find the optimal control for the following approximate dynamics

$$\dot{V} = \frac{\kappa^2 + \lambda}{\kappa^2 + 2\lambda} \alpha V - \frac{\kappa\lambda(2V - T_b)}{(\kappa^2 + 2\lambda)}. \quad (\text{S1})$$

where $\alpha = \dot{\lambda}/\lambda$ is the rate of varying the stiffness. The work rate during the isothermal process is

$$\dot{W} = \alpha V. \quad (\text{S2})$$

To maximize the output work

$$W_{\text{out}} = -W = \int_0^\tau \alpha V dt, \quad (\text{S3})$$

* chenjinfu@pku.edu.cn

† htquan@pku.edu.cn

we introduce the Lagrange multipliers ψ_V and ψ_λ and construct the Lagrangian

$$\mathcal{L} = -\alpha V + \psi_V \left[\frac{\kappa^2 + \lambda}{\kappa^2 + 2\lambda} \alpha V - \frac{\kappa\lambda(2V - T_b)}{\kappa^2 + 2\lambda} - \dot{V} \right] + \psi_\lambda(\alpha\lambda - \dot{\lambda}). \quad (\text{S4})$$

When the control parameters are varied under control constraints, it is more convenient to define the pseudo-Hamiltonian $\mathcal{H} = \mathcal{H}(V, \lambda, \psi_V, \psi_\lambda, \alpha, T_b)$ as [1]

$$\mathcal{H} = \psi_V \dot{V} + \psi_\lambda \dot{\lambda} + \mathcal{L} \quad (\text{S5})$$

$$= -\alpha V + \psi_V \left[\frac{\kappa^2 + \lambda}{\kappa^2 + 2\lambda} \alpha V - \frac{\kappa\lambda(2V - T_b)}{\kappa^2 + 2\lambda} \right] + \psi_\lambda \alpha, \quad (\text{S6})$$

where the state variables are V and λ , the corresponding costate variables are ψ_V and ψ_λ , and the control parameters are the rate of stiffness change α and the bath temperature T_b . The evolution of the state variables is generated by

$$\dot{V} = \frac{\partial \mathcal{H}}{\partial \psi_V} = \frac{\kappa^2 + \lambda}{\kappa^2 + 2\lambda} \alpha V - \frac{\kappa\lambda(2V - T_b)}{\kappa^2 + 2\lambda}, \quad (\text{S7})$$

$$\dot{\lambda} = \frac{\partial \mathcal{H}}{\partial \psi_\lambda} = \alpha\lambda. \quad (\text{S8})$$

The evolution of the costate variables is generated by

$$\dot{\psi}_V = -\frac{\partial \mathcal{H}}{\partial V} = \alpha \left[1 - \frac{(\kappa^2 + \lambda) \psi_V}{\kappa^2 + 2\lambda} \right] + \frac{2\kappa\lambda\psi_V}{\kappa^2 + 2\lambda}, \quad (\text{S9})$$

$$\dot{\psi}_\lambda = -\frac{\partial \mathcal{H}}{\partial \lambda} = \alpha \left[\frac{\kappa^2 V \psi_V}{(\kappa^2 + 2\lambda)^2} - \psi_\lambda \right] - \frac{\kappa^3 (T_b - 2V) \psi_V}{(\kappa^2 + 2\lambda)^2}. \quad (\text{S10})$$

The control parameters are varied to possibly maximize the pseudo-Hamiltonian \mathcal{H} . We compute its derivatives on the control parameters. The control of bath temperature is determined by

$$\frac{\partial \mathcal{H}}{\partial T_b} = \frac{\kappa\lambda\psi_V}{\kappa^2 + 2\lambda}, \quad (\text{S11})$$

which corresponds to a bang-bang control $T_b = T_H$ for $\psi_V > 0$ and T_L for $\psi_V < 0$. The control of the stiffness change rate α is determined from

$$\frac{\partial \mathcal{H}}{\partial \alpha} = \lambda\psi_\lambda + \frac{V(\kappa^2 + \lambda)\psi_V}{\kappa^2 + 2\lambda} - V, \quad (\text{S12})$$

which does not depend on α . The control of the rate of stiffness change corresponds to a singular control.

A. Isothermal processes

We solve the singular control in the following. The pseudo-Hamiltonian \mathcal{H} remains constant during the singular control

$$\frac{d}{dt} \mathcal{H}(V, \lambda, \psi_V, \psi_\lambda, \alpha, T_b) = \dot{V} \frac{\partial \mathcal{H}}{\partial V} + \dot{\lambda} \frac{\partial \mathcal{H}}{\partial \lambda} + \dot{\psi}_V \frac{\partial \mathcal{H}}{\partial \psi_V} + \dot{\psi}_\lambda \frac{\partial \mathcal{H}}{\partial \psi_\lambda} + \dot{\alpha} \frac{\partial \mathcal{H}}{\partial \alpha} + \dot{T}_b \frac{\partial \mathcal{H}}{\partial T_b}. \quad (\text{S13})$$

The first four terms diminish according to the canonical evolution equations of the state variables (Eqs. (S7) and (S8)) and the costate variables (Eqs. (S9) and (S10)). The last term is also zero since the control of bath temperature is bang-bang. Thus, the singular control requires that

$$\frac{\partial \mathcal{H}}{\partial \alpha} = \lambda\psi_\lambda + \frac{V(\kappa^2 + \lambda)\psi_V}{\kappa^2 + 2\lambda} - V = 0. \quad (\text{S14})$$

This quantity remains to be zero during the singular control, therefore,

$$\frac{d}{dt} \left(\lambda \psi_\lambda + \frac{V(\kappa^2 + \lambda) \psi_V}{\kappa^2 + 2\lambda} - V \right) = 0. \quad (\text{S15})$$

Plugging Eqs. (S9) and (S10) into Eq. (S15), we obtain

$$\psi_V (\lambda T_b + 2\kappa^2 V) + (\kappa^2 + 2\lambda) (2V - T_b) = 0. \quad (\text{S16})$$

Similarly, we have

$$\frac{d}{dt} [\psi_V (\lambda T_b + 2\kappa^2 V) + (\kappa^2 + 2\lambda) (2V - T_b)] = 0. \quad (\text{S17})$$

Plugging Eqs. (S9) and (S10) into Eq. (S17), we obtain

$$\psi_V \left[\lambda T_b \left(\alpha \frac{\kappa^2 - \lambda}{\kappa^2 + 2\lambda} + 2\kappa \frac{\kappa^2 + \lambda}{\kappa^2 + 2\lambda} \right) + 2\alpha \kappa^2 V \frac{\kappa^2 - 2\lambda}{\kappa^2 + 2\lambda} \right] + T_b [\alpha (\lambda - \kappa^2) + 2\kappa \lambda] + 2V [\alpha (3\kappa^2 + \lambda) - 2\kappa \lambda] = 0. \quad (\text{S18})$$

We solve ψ_V and ψ_λ from Eqs. (S14) and (S16) as

$$\psi_V = \frac{(\kappa^2 + 2\lambda) (T_b - 2V)}{\lambda T_b + 2\kappa^2 V}, \quad (\text{S19})$$

$$\psi_\lambda = \frac{V [2V (2\kappa^2 + \lambda) - \kappa^2 T_b]}{\lambda (\lambda T_b + 2\kappa^2 V)}, \quad (\text{S20})$$

Together with Eq. (S18), we obtain the solution to the control parameter

$$\alpha = \frac{\kappa \lambda (2V - T_b) [2\kappa^2 V + (\kappa^2 + 2\lambda) T_b]}{V [4\kappa^4 V + 6\kappa^2 \lambda V + (\kappa^2 + 2\lambda) \lambda T_b]}. \quad (\text{S21})$$

The conserved pseudo-Hamiltonian is obtained

$$\mathcal{H} = \frac{\kappa \lambda (T_b - 2V)^2}{\lambda T_b + 2\kappa^2 V}. \quad (\text{S22})$$

We can solve the stiffness as

$$\lambda = \frac{2\kappa^2 V \mathcal{H}}{\kappa (T_b - 2V)^2 - T_b \mathcal{H}}. \quad (\text{S23})$$

Substituting Eq. (S21) into Eqs. (S7) and (S8), we obtain

$$\dot{V} = -\frac{\kappa^3 \lambda (T_b - 2V)^2}{2\lambda^2 T_b + \kappa^2 \lambda (T_b + 6V) + 4\kappa^4 V}, \quad (\text{S24})$$

$$\dot{\lambda} = \frac{\kappa \lambda^2 (2V - T_b) [2\kappa^2 V + T_b (\kappa^2 + 2\lambda)]}{V [4\kappa^4 V + 6\kappa^2 \lambda V + T_b (\kappa^2 + 2\lambda) \lambda]}. \quad (\text{S25})$$

We determine the work in the isothermal process as

$$\begin{aligned}
W_{\text{iso}} &= \int_{\lambda_i}^{\lambda_f} V \frac{d\lambda}{\lambda} \\
&= \int_{V_i}^{V_f} \frac{\kappa T_b^2 - \mathcal{H}T_b - 4\kappa V^2}{\kappa (T_b - 2V)^2 - \mathcal{H}T_b} dV \\
&= \left[-\frac{1}{2}T_b \ln \left(\kappa (T_b - 2V)^2 - \mathcal{H}T_b \right) - \sqrt{\frac{\mathcal{H}T_b}{\kappa}} \tanh^{-1} \left(\sqrt{\frac{\kappa}{\mathcal{H}T_b}} (T_b - 2V) \right) - V \right] \Big|_{V=V_i}^{V_f}. \tag{S26}
\end{aligned}$$

The operation time of the isothermal process is

$$\begin{aligned}
\tau_{\text{iso}} &= \int_{V_i}^{V_f} \frac{dV}{\dot{V}} \\
&= - \int_{V_i}^{V_f} \frac{2\kappa^2 (T_b - 2V)^3 - 3\kappa\mathcal{H} (T_b - 2V)^2 + \mathcal{H}^2 T_b}{\kappa\mathcal{H} (T_b - 2V) (\kappa (T_b - 2V)^2 - \mathcal{H}T_b)} dV \\
&= \left[-\frac{\ln \left(\kappa (T_b - 2V)^2 - \mathcal{H}T_b \right)}{2\kappa} - \frac{\ln (2V - T_b)}{2\kappa} - \sqrt{\frac{T_b}{\kappa\mathcal{H}}} \tanh^{-1} \left(\sqrt{\frac{\kappa}{\mathcal{H}T_b}} (T_b - 2V) \right) - \frac{2V}{\mathcal{H}} \right] \Big|_{V=V_i}^{V_f}. \tag{S27}
\end{aligned}$$

B. Switchings: connecting processes

The Pontryagin maximum principle requires that in the optimal control the pseudo-Hamiltonian remains constant [1]. To construct cycles, we need to find some switchings to connect the two singular isothermal processes at temperatures $T_b = T_L$ and T_H . In the switchings, the pseudo-Hamiltonian \mathcal{H} remains unchanged. The switchings can be realized by simultaneously changing T_b and λ instantaneously, where the heat exchanged can be neglected. The evolution of the state variables and costate variables during the switchings is reduced to

$$\dot{V} = \frac{\kappa^2 + \lambda}{\kappa^2 + 2\lambda} \alpha V, \tag{S28}$$

$$\dot{\lambda} = \alpha \lambda, \tag{S29}$$

$$\dot{\psi}_V = \alpha \left[1 - \frac{(\kappa^2 + \lambda) \psi_V}{\kappa^2 + 2\lambda} \right], \tag{S30}$$

$$\dot{\psi}_\lambda = \alpha \left[\frac{\kappa^2 V \psi_V}{(\kappa^2 + 2\lambda)^2} - \psi_\lambda \right]. \tag{S31}$$

Thus the values of the potential energy V and its costate variable ψ_V at the beginning and the end of the switchings should satisfy

$$\frac{V_f \sqrt{\kappa^2 + 2\lambda_f}}{\lambda_i} = \frac{V_i \sqrt{2\lambda_i + \kappa^2}}{\lambda_i}, \tag{S32}$$

$$\frac{\lambda_f (\psi_{V_f} - 2) - \kappa^2}{\sqrt{\kappa^2 + 2\lambda_f}} = \frac{\lambda_i (\psi_{V_i} - 2) - \kappa^2}{\sqrt{\kappa^2 + 2\lambda_i}}. \tag{S33}$$

We calculate the work of the connecting process as

$$\begin{aligned}
W_{\text{con}} &= \int_{\lambda_i}^{\lambda_f} \frac{d\lambda}{\lambda} V \\
&= \frac{V_i}{\lambda_i} \sqrt{\kappa^2 + 2\lambda_i} \int_{\lambda_i}^{\lambda_f} \frac{d\lambda}{\sqrt{\kappa^2 + 2\lambda}} \\
&= \frac{V_i}{\lambda_i} \sqrt{\kappa^2 + 2\lambda_i} (\sqrt{\kappa^2 + 2\lambda_f} - \sqrt{\kappa^2 + 2\lambda_i}). \tag{S34}
\end{aligned}$$

Notice that the pseudo-Hamiltonian \mathcal{H} should be conserved in the optimal control of the whole cycle. We will use the conservation of \mathcal{H} to determine the switching.

C. Construction of heat engine cycles

Using the conservation of \mathcal{H} and the control constraints of the stiffness $\lambda_L \leq \lambda \leq \lambda_H$, we find two switchings that can be realized by using the low and the high stiffness constraints λ_L and λ_H respectively. We first consider the switching by increasing λ to λ_H . This happens during the cold isothermal process by simultaneously changing the stiffness from λ_2 to λ_H and the bath temperature from T_L to T_H . The conservation of \mathcal{H} leads to

$$\mathcal{H} = \frac{\kappa\lambda(T_L - 2V_2)^2}{\lambda T_L + 2\kappa^2 V_2} = -\psi_{V3} \frac{\kappa\lambda_H(2V_3 - T_H)}{\kappa^2 + 2\lambda_H}, \quad (\text{S35})$$

where ψ_{V3} is given by Eq. (S19). We solve this connecting process by using the fact that V_3 and ψ_{V3} are related to V_2 and ψ_{V2} according to Eqs. (S32) and (S33).

Similarly, the other switching by decreasing λ to λ_L happens during the hot isothermal process by simultaneously changing the stiffness from λ_5 to λ_L and the bath temperature from T_H to T_L . The conservation of \mathcal{H} leads to

$$\mathcal{H} = \frac{\kappa\lambda_5(T_H - 2V_5)^2}{\lambda_5 T_H + 2\kappa^2 V_5} = -\psi_{V6} \frac{\kappa\lambda_L(2V_6 - T_L)}{\kappa^2 + 2\lambda_L}. \quad (\text{S36})$$

Given specific λ_L , we identify the maximum \mathcal{H} such that point 6 approaches to point 1 on the cold isothermal curve. When \mathcal{H} is larger than the maximum value, the left switching connects the two isothermal processes directly without reaching λ_L .

We determine the maximum \mathcal{H} from the conservation of pseudo-Hamiltonian

$$\mathcal{H} = \frac{\kappa\lambda_5(T_H - 2V_5)^2}{\lambda_5 T_H + 2\kappa^2 V_5} = \frac{\kappa\lambda_L(T_L - 2V_1)^2}{\lambda_L T_L + 2\kappa^2 V_1}. \quad (\text{S37})$$

Points 1 and 5 are on the cold and the hot isothermal curves respectively, and they satisfy the relation of the switching

$$\frac{V_1}{\lambda_L} \sqrt{\kappa^2 + 2\lambda_L} = \frac{V_5}{\lambda_5} \sqrt{\kappa^2 + 2\lambda_5}, \quad (\text{S38})$$

$$\frac{\lambda_L(\psi_{V1} - 2) - \kappa^2}{\sqrt{\kappa^2 + 2\lambda_L}} = \frac{\lambda_5(\psi_{V5} - 2) - \kappa^2}{\sqrt{\kappa^2 + 2\lambda_5}}, \quad (\text{S39})$$

and ψ_{V1} and ψ_{V5} are related to V_1 and V_5 according to Eq. (S19). Thus the maximum \mathcal{H} is determined by λ_L , T_L and T_H , but we only obtain the numerical results in generic damped situation. We will show analytical results of the maximum \mathcal{H} in the underdamped and the overdamped limits in Sec. II and Sec. III, respectively. The output power of the maximum- \mathcal{H} cycle is

$$P = -\frac{W_I + W_{II} + W_{IV} + W_V}{\tau_I + \tau_{III} + \tau_{IV}}, \quad (\text{S40})$$

where we evaluate the work W_I and W_{IV} of two isothermal processes by Eq. (S26), the work W_{II} and W_V of the two connecting processes by Eq. (S34), the duration τ_I and τ_{IV} of two isothermal processes by Eq. (S27), the duration of the isochoric relaxation by

$$\tau_{III} = \frac{\kappa^2 + 2\lambda}{\kappa\lambda} \ln \frac{2V_3 - T_H}{2V_4 - T_H}. \quad (\text{S41})$$

As an illustration, we show cycle diagrams λ - V in Fig. S1 under the parameters $T_L = 0.9$, $T_H = 1$, $\lambda_L = 0.5$, $\lambda_H = 1$, and $\kappa = 1$. The control of a whole cycle is determined by \mathcal{H} . Increasing the output power is converted to finding the cycle with larger \mathcal{H} . For larger \mathcal{H} , the path of the process VI becomes shorter. For the maximum \mathcal{H} , process VI diminishes and point 6 approaches to point 1, as shown in Fig. S1(b). In the following, we focus on maximum- \mathcal{H} cycles for given control constraints. To improve the output power, we need to construct the maximum- \mathcal{H} cycles with appropriate friction coefficient κ .

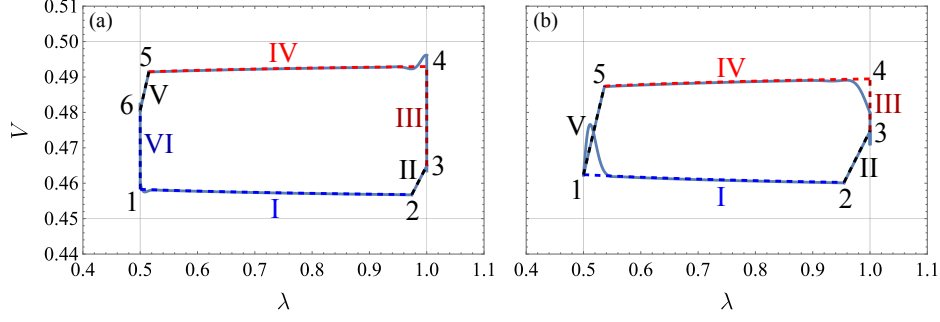


Figure S1. Diagrams of heat-engine cycles. (a) $\mathcal{H} = 10^{-4}$ (non-maximum- \mathcal{H}) and (b) $\mathcal{H} = 2.246 \times 10^{-4}$ (maximum- \mathcal{H}). The friction coefficient is $\kappa = 1$, and the control constraints $T_L = 0.9$, $T_H = 1$, $\lambda_L = 0.5$ and $\lambda_H = 1$ are depicted by the horizontal and vertical gray lines. The dashed curves represent the estimated evolution, while the solid curves are the exact evolution for the limit cycles.

II. OPTIMIZATION IN UNDERDAMPED LIMIT

We discuss the optimization of the cycle in the underdamped limit $\kappa^2 \ll \lambda$. The pseudo-Hamiltonian (S6) becomes

$$\mathcal{H} = -\alpha V + \psi_V \left[\frac{1}{2} \alpha V - \kappa \left(V - \frac{T_b}{2} \right) \right] + \psi_\lambda \lambda \alpha. \quad (\text{S42})$$

The evolution of the state variables and costate variables is given by

$$\dot{V} = \frac{\partial \mathcal{H}}{\partial \psi_V} = \frac{1}{2} \alpha V - \kappa \left(V - \frac{T_b}{2} \right), \quad (\text{S43})$$

$$\dot{\lambda} = \frac{\partial \mathcal{H}}{\partial \psi_\lambda} = \alpha \lambda, \quad (\text{S44})$$

$$\dot{\psi}_V = -\frac{\partial \mathcal{H}}{\partial V} = \alpha - \psi_V \left(\frac{\alpha}{2} - \kappa \right), \quad (\text{S45})$$

$$\dot{\psi}_\lambda = -\frac{\partial \mathcal{H}}{\partial \lambda} = -\alpha \psi_\lambda. \quad (\text{S46})$$

The control of bath temperature is determined by

$$\frac{\partial \mathcal{H}}{\partial T_b} = \frac{\kappa \psi_V}{2}, \quad (\text{S47})$$

which corresponds to a bang-bang control $T_b = T_H$ for $\psi_V > 0$ and T_L for $\psi_V < 0$. The control of the stiffness change rate α is determined from

$$\frac{\partial \mathcal{H}}{\partial \alpha} = \psi_\lambda \lambda + \left(\frac{\psi_V}{2} - 1 \right) V. \quad (\text{S48})$$

We consider the singular control

$$\frac{\partial \mathcal{H}}{\partial \alpha} = \psi_\lambda \lambda + \left(\frac{\psi_V}{2} - 1 \right) V = 0. \quad (\text{S49})$$

This quantity remains to be zero during the singular control, therefore,

$$\frac{d}{dt} \left[\psi_\lambda \lambda + \left(\frac{\psi_V}{2} - 1 \right) V \right] = 0. \quad (\text{S50})$$

Plugging Eqs. (S45) and (S80) into Eq. (S50), we obtain

$$\frac{1}{2} \kappa T_b \left(\frac{\psi_V}{2} - 1 \right) + \kappa V = 0. \quad (\text{S51})$$

Similarly, we have

$$\frac{d}{dt} \left[\frac{1}{2} \kappa T_b \left(\frac{\psi_V}{2} - 1 \right) + \kappa V \right] = 0, \quad (\text{S52})$$

which leads to

$$\alpha \left[V - \frac{1}{4} T_b (\psi_V - 2) \right] + \kappa \left[\frac{1}{2} T_b (\psi_V + 2) - 2V \right] = 0. \quad (\text{S53})$$

We solve ψ_V and ψ_λ from Eqs. (S49) and (S51) as

$$\psi_V = 2 - \frac{4V}{T_b}, \quad (\text{S54})$$

$$\psi_\lambda = \frac{2V^2}{\lambda T_b}. \quad (\text{S55})$$

We further use Eq. (S53), and obtain the singular optimal control satisfying

$$\frac{\dot{\lambda}}{\lambda} = \alpha = \kappa \left(2 - \frac{T_b}{V} \right). \quad (\text{S56})$$

Together with the evolution equation (S43), we find that V and α remains constant in the singular control, and λ is varied in the exponential protocol. Such exponential protocols have been found as the optimal protocols in the underdamped limit [2–5].

Substituting Eqs. (S54) and (S55) into Eq. (S42), the pseudo-Hamiltonian is explicitly

$$\mathcal{H} = \frac{\kappa (T_b - 2V)^2}{T_b}, \quad (\text{S57})$$

which is consistent with Eq. (S22) by taking the underdamped limit $\kappa^2 \ll \lambda$. From Eq. (S57), we obtain the potential energy is constant in the singular control

$$V = \frac{1}{2} (T_b \pm \sqrt{\frac{T_b \mathcal{H}}{\kappa}}). \quad (\text{S58})$$

We next consider the switchings between the two isothermal curves $T_b = T_L$ and T_H , and construct the maximum- \mathcal{H} cycle in the underdamped limit.

Construction of heat-engine cycles

We construct heat-engine cycles in the underdamped limit. In the switchings, the stiffness is rapidly changed and the heat exchange can be neglected. The differential equations (S43) and (S45) are reduced to

$$\dot{V} = \frac{1}{2} \alpha V, \quad (\text{S59})$$

$$\dot{\psi}_V = \alpha \left(1 - \frac{\psi_V}{2} \right). \quad (\text{S60})$$

According to Eq. (S59), the work in a connecting process is obtained as

$$W_{\text{con}}^{\text{over}} = \int_0^{\tau_{\text{con}}} \alpha V dt = 2(V_f - V_i). \quad (\text{S61})$$

We determine the maximum- \mathcal{H} cycle from the conservation of the pseudo-Hamiltonian in the whole cycle

$$\mathcal{H} = \frac{\kappa (T_H - 2V_5)^2}{T_H} = \frac{\kappa (T_L - 2V_1)^2}{T_L}. \quad (\text{S62})$$

Points 1 and 5 are on the cold and the hot isothermal curves respectively. According to Eqs. (S59) and (S60), the two points satisfy the relation of the switching

$$\frac{V_1}{\sqrt{\lambda_L}} = \frac{V_5}{\sqrt{\lambda_5}}, \quad (\text{S63})$$

$$\sqrt{\lambda_L}(\psi_{V1} - 2) = \sqrt{\lambda_5}(\psi_{V5} - 2). \quad (\text{S64})$$

We obtain the solution

$$V_1 = \frac{1}{4}(T_L + \sqrt{T_H T_L}), \quad (\text{S65})$$

$$V_5 = \frac{1}{4}(T_H + \sqrt{T_H T_L}), \quad (\text{S66})$$

$$\mathcal{H} = \frac{\kappa}{4}(\sqrt{T_H} - \sqrt{T_L})^2. \quad (\text{S67})$$

The rate of the stiffness change is

$$\alpha = \begin{cases} 2\kappa \frac{\sqrt{T_H} - \sqrt{T_L}}{\sqrt{T_H} + \sqrt{T_L}}, & T_b = T_L \\ -2\kappa \frac{\sqrt{T_H} - \sqrt{T_L}}{\sqrt{T_H} + \sqrt{T_L}}, & T_b = T_H \end{cases} \quad (\text{S68})$$

Since V remains constant in the singular control in the underdamped limit, we obtain $V_2 = V_1$ and $V_4 = V_5$, and the isochoric process III also diminishes in the maximum- \mathcal{H} cycle, i.e., $V_3 = V_5$.

The work and the operation time of each process in the underdamped limit can be easily calculated. Here we just list the results in the following. The performed work of each process is

$$W_{\text{I}} = V_1 \ln \frac{\lambda_2}{\lambda_L} = \frac{1}{4}(T_L + \sqrt{T_H T_L}) \ln \frac{\lambda_2}{\lambda_L}, \quad (\text{S69})$$

$$W_{\text{II}} = 2V_3 - 2V_2 = \frac{1}{2}(T_H - T_L), \quad (\text{S70})$$

$$W_{\text{IV}} = V_4 \ln \frac{\lambda_5}{\lambda_H} = -\frac{1}{4}(T_H + \sqrt{T_H T_L}) \ln \frac{\lambda_2}{\lambda_L}, \quad (\text{S71})$$

$$W_{\text{V}} = 2V_1 - 2V_5 = -\frac{1}{2}(T_H - T_L), \quad (\text{S72})$$

and the operation time is

$$\tau_{\text{I}} = \tau_{\text{IV}} = \frac{\sqrt{T_H} + \sqrt{T_L}}{2\kappa(\sqrt{T_H} - \sqrt{T_L})} \ln \frac{\lambda_2}{\lambda_L}, \quad (\text{S73})$$

$$\tau_{\text{III}} = 0. \quad (\text{S74})$$

According to Eq. (S40), we obtain the maximum output power in the underdamped limit [3, 5]

$$P_{\text{under}}^* = \frac{\kappa}{4}(\sqrt{T_H} - \sqrt{T_L})^2. \quad (\text{S75})$$

which does not depend on the stiffness constraints. The maximum output power (S75) in the underdamped limit is proportional to κ .

III. OPTIMIZATION IN OVERDAMPED LIMIT

We discuss the optimization of the cycle in the overdamped limit $\kappa^2 \gg \lambda$. The pseudo-Hamiltonian (S6) becomes

$$\mathcal{H} = -\alpha V + \psi_V \left[\alpha V - \frac{\lambda(2V - T_b)}{\kappa} \right] + \psi_\lambda \lambda \alpha. \quad (\text{S76})$$

The evolution of the state variables and costate variables is given by

$$\dot{V} = \frac{\partial \mathcal{H}}{\partial \psi_V} = \alpha V - \frac{\lambda(2V - T_b)}{\kappa}, \quad (\text{S77})$$

$$\dot{\lambda} = \frac{\partial \mathcal{H}}{\partial \psi_\lambda} = \alpha \lambda, \quad (\text{S78})$$

$$\dot{\psi}_V = -\frac{\partial \mathcal{H}}{\partial V} = \psi_V \left(\frac{2\lambda}{\kappa} - \alpha \right) + \alpha, \quad (\text{S79})$$

$$\dot{\psi}_\lambda = -\frac{\partial \mathcal{H}}{\partial \lambda} = -\frac{\alpha \kappa \psi_\lambda + \psi_V (T_b - 2V)}{\kappa}. \quad (\text{S80})$$

The control of bath temperature is determined by

$$\frac{\partial \mathcal{H}}{\partial T_b} = \frac{\lambda}{\kappa} \psi_V, \quad (\text{S81})$$

which corresponds to a bang-bang control $T_b = T_H$ for $\psi_V > 0$ and T_L for $\psi_V < 0$. The control of the stiffness change rate α is determined from

$$\frac{\partial \mathcal{H}}{\partial \alpha} = \lambda \psi_\lambda + V (\psi_V - 1). \quad (\text{S82})$$

We consider the singular control

$$\frac{\partial \mathcal{H}}{\partial \alpha} = \lambda \psi_\lambda + V (\psi_V - 1) = 0. \quad (\text{S83})$$

This quantity remains to be zero during the singular control, therefore,

$$\frac{d}{dt} [\lambda \psi_\lambda + V (\psi_V - 1)] = 0. \quad (\text{S84})$$

Plugging Eqs. (S77) and (S78) into Eq. (S84), we obtain

$$2V (\psi_V + 1) - T_b = 0 \quad (\text{S85})$$

Similarly, we have

$$\frac{d}{dt} [2V (\psi_V + 1) - T_b] = 0, \quad (\text{S86})$$

which leads to

$$\alpha \kappa [T_b - 2V (\psi_V + 3)] - 2\lambda T_b (\psi_V + 1) + 4\lambda V = 0. \quad (\text{S87})$$

We solve ψ_V and ψ_λ from Eqs. (S83) and (S85) as

$$\psi_V = \frac{T_b}{2V} - 1, \quad (\text{S88})$$

$$\psi_\lambda = \frac{2V}{\lambda} - \frac{T_b}{2\lambda}, \quad (\text{S89})$$

We further use Eq. (S87) and obtain the singular optimal control as

$$\alpha = \frac{\lambda}{\kappa} \left(1 - \frac{T_b^2}{4V^2} \right). \quad (\text{S90})$$

The differential equations for the optimal control are

$$\dot{\lambda} = \frac{\lambda^2}{\kappa} \left(1 - \frac{T_b^2}{4V^2} \right), \quad (\text{S91})$$

$$\dot{V} = -\frac{\lambda}{\kappa V} \left(V - \frac{T_b}{2} \right)^2. \quad (\text{S92})$$

Under the initial condition $\lambda(0) = \lambda_0$ and $V(0) = V_0$, we obtain the solution

$$V(t) = V_0 - \frac{\lambda_0 t (T_b - 2V_0)^2}{4\kappa V_0}, \quad (\text{S93})$$

$$\lambda(t) = \frac{\kappa \lambda_0 [4\kappa V_0^2 - \lambda_0 t (T_b - 2V_0)^2]}{[\lambda_0 t (T_b - 2V_0) + 2\kappa V_0]^2}. \quad (\text{S94})$$

which coincides with the control scheme obtained in Refs. [6, 7].

Substituting Eqs. (S88) and (S89) into Eq. (S76), the pseudo-Hamiltonian is explicitly

$$\mathcal{H} = \frac{\lambda (T_b - 2V)^2}{2\kappa V}. \quad (\text{S95})$$

This expression is consistent with Eq. (S22) by taking the overdamped limit $\kappa^2 \gg \lambda$. Therefore, the potential energy is related to the stiffness as

$$V = \frac{T_b}{2} + \frac{\kappa \mathcal{H}}{4\lambda} \left(1 \pm \sqrt{\frac{4\lambda T_b}{\kappa \mathcal{H}} + 1} \right). \quad (\text{S96})$$

The work in an isothermal process can be obtained as

$$\begin{aligned} W_{\text{iso}}^{\text{over}} &= \int_{\lambda_i}^{\lambda_f} \frac{V}{\lambda} d\lambda \\ &= \int_{V_i}^{V_f} \frac{T_b + 2V}{T_b - 2V} dV \\ &= V_i - V_f + T_b \ln \frac{2V_i - T_b}{2V_f - T_b}. \end{aligned} \quad (\text{S97})$$

The operation time is

$$\begin{aligned} \tau_{\text{iso}}^{\text{over}} &= \int_{V_i}^{V_f} \frac{dV}{\dot{V}} \\ &= - \int_{V_i}^{V_f} \frac{4\kappa V}{\lambda (2V - T_b)^2} dV \\ &= 2 \frac{V_i - V_f}{\mathcal{H}}. \end{aligned} \quad (\text{S98})$$

Thus, we obtain the work and operation time for processes I and IV in the overdamped limit.

Construction of heat-engine cycles

In the switchings, the stiffness is suddenly changed and the heat exchange can be neglected. The differential equations (S77) and (S79) are reduced to

$$\dot{V} = \alpha V, \quad (\text{S99})$$

$$\dot{\psi}_V = (1 - \psi_V)\alpha. \quad (\text{S100})$$

According to Eq. (S99), the work in a connecting process is obtained as

$$W_{\text{con}}^{\text{over}} = \int_0^{\tau_{\text{con}}} \alpha V dt = V_f - V_i. \quad (\text{S101})$$

When the stiffness is switched to λ_H , an isochoric relaxation process follows

$$\dot{V} = -\frac{\lambda_H(2V - T_H)}{\kappa}, \quad (\text{S102})$$

$$\dot{\psi}_V = \psi_V \frac{2\lambda_H}{\kappa}. \quad (\text{S103})$$

We first calculate the left switching of the maximum- \mathcal{H} cycle in the overdamped limit. According to Eqs. (S99) and (S100), the two boundary points 1 and 5 satisfy

$$\frac{V_5}{\lambda_5} = \frac{V_1}{\lambda_L}, \quad (\text{S104})$$

$$(1 - \psi_{V_5})\lambda_5 = (1 - \psi_{V_1})\lambda_L, \quad (\text{S105})$$

where ψ_{V_1} and ψ_{V_5} are related to V_1 and V_5 by Eq. (S88). The two points are located on two isothermal curves, and the conservation of \mathcal{H} leads to

$$\mathcal{H} = \frac{\lambda_L(T_L - 2V_1)^2}{2\kappa V_1} = \frac{\lambda_5(T_H - 2V_5)^2}{2\kappa V_5}. \quad (\text{S106})$$

From Eqs. (S104)-(S106), we obtain the solution of the left switching for the maximum- \mathcal{H} cycle

$$\mathcal{H} = \frac{(T_H - T_L)^2 \lambda_L}{4(T_H + 3T_L)\kappa}, \quad (\text{S107})$$

$$V_1 = \frac{1}{8}(T_H + 3T_L), \quad (\text{S108})$$

$$\psi_{V_1} = -\frac{T_H - T_L}{T_H + 3T_L}, \quad (\text{S109})$$

$$\lambda_5 = \frac{3T_H + T_L}{T_H + 3T_L} \lambda_L, \quad (\text{S110})$$

$$V_5 = \frac{1}{8}(3T_H + T_L), \quad (\text{S111})$$

$$\psi_{V_5} = \frac{T_H - T_L}{3T_H + T_L}. \quad (\text{S112})$$

To achieve large \mathcal{H} , we can possibly choose large λ_L , but λ_5 should be less than λ_H , which gives

$$\lambda_L \leq \frac{T_H + 3T_L}{3T_H + T_L} \lambda_H, \quad (\text{S113})$$

and the pseudo-Hamiltonian is less than

$$\mathcal{H} \leq \frac{(T_H - T_L)^2 \lambda_H}{4(3T_H + T_L)\kappa}. \quad (\text{S114})$$

We next solve the right switching with given \mathcal{H} . The potential energy and the stiffness for the points 2 and 3 satisfy

$$\mathcal{H} = \frac{\lambda_2 (T_L - 2V_2)^2}{2\kappa V_2} = -\psi_{V_3} \frac{\lambda_H}{\kappa} (2V_3 - T_H), \quad (\text{S115})$$

$$\frac{V_3}{\lambda_H} = \frac{V_2}{\lambda_2}, \quad (\text{S116})$$

$$(1 - \psi_{V_3})\lambda_H = (1 - \psi_{V_2})\lambda_2, \quad (\text{S117})$$

$$\psi_{V_2} = \frac{T_L}{2V_2} - 1. \quad (\text{S118})$$

We eliminate V_3 and ψ_{V_3} and obtain

$$\mathcal{H} = \left[\left(2 - \frac{T_L}{2V_2}\right) \frac{\lambda_2}{\lambda_H} - 1 \right] \frac{\lambda_H}{\kappa} \left(2 \frac{\lambda_H V_2}{\lambda_2} - T_H\right), \quad (\text{S119})$$

$$V_2 = \frac{T_L}{2} + \frac{\kappa \mathcal{H}}{4\lambda_2} \left(1 - \sqrt{\frac{4\lambda T_L}{\kappa \mathcal{H}} + 1}\right). \quad (\text{S120})$$

We do not find simple algebra expressions of V_2 and λ_2 . However, Eqs. (S119) and (S120) have real solutions only when \mathcal{H} is less than a maximum value $\mathcal{H}_{\max}^{\text{over}}$. To evaluate $\mathcal{H}_{\max}^{\text{over}}$, we first eliminate λ_2 and obtain the solution $V_2 = T_H \chi$, where $\chi > T_L/(2T_H)$ is the root of a fourth-order polynomial

$$f\left(\chi, \frac{\kappa \mathcal{H}}{\lambda_H T_H}\right) = 0, \quad (\text{S121})$$

where the polynomial is explicitly

$$f(\chi, \phi) = \phi^2 [(\theta - 4\chi) - (\theta - 2\chi)^2] + \phi(\theta - 2\chi)^2(1 - \theta + 4\chi) - (\theta - 2\chi)^4. \quad (\text{S122})$$

We use $\theta = T_L/T_H$ to denote the temperature ratio. If the polynomial has a real root satisfying $\chi > T_L/(2T_H)$, the maximum value $f(\chi^*, \phi)$ on $\chi > T_L/(2T_H)$ should be positive. Thus, the maximum point satisfies

$$f(\chi^*, \phi) \geq 0, \quad (\text{S123})$$

$$\left. \frac{\partial f}{\partial \chi} \right|_{\chi=\chi^*} = 0. \quad (\text{S124})$$

Then we solve the above formulas with the equality and obtain $\phi(\theta)$ as a positive root of a third-order polynomial

$$\phi^3 + (11 - 3\theta)\phi^2 + (3\theta^2 + 14\theta - 1)\phi - (1 - \theta)^2\theta = 0. \quad (\text{S125})$$

The positive root is explicitly

$$\phi(\theta) = \frac{1}{3} \sqrt[3]{\Upsilon(\theta)} + \frac{4}{3} \frac{(31 - 27\theta)}{\sqrt[3]{\Upsilon(\theta)}} + \theta - \frac{11}{3}, \quad (\text{S126})$$

where

$$\Upsilon(\theta) = -\frac{729\theta^2}{2} + 1809\theta - \frac{2761}{2} + \frac{3}{2}i\sqrt{3(1-\theta)(27\theta+5)^3}. \quad (\text{S127})$$

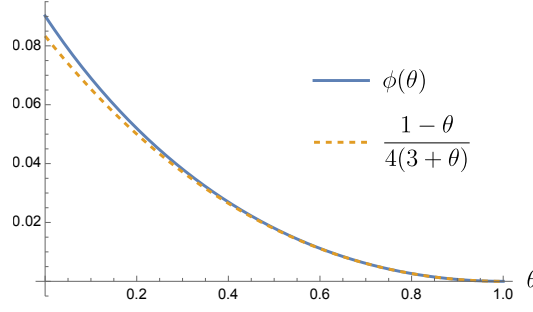


Figure S2. Comparison of the precise and approximate results of the maximum power (Eq. (S137)) in the overdamped limit.

The maximum value $\mathcal{H}_{\text{over}}^{\text{max}}$ is represented as

$$\mathcal{H}_{\text{over}}^{\text{max}} = \frac{\lambda_H T_H}{\kappa} \phi\left(\frac{T_L}{T_H}\right). \quad (\text{S128})$$

According to Eqs. (S97) and (S101), we obtain the expression of the performed work for each process as

$$W_{\text{I}} = V_1 - V_2 + T_L \ln \frac{2V_1 - T_L}{2V_2 - T_L}, \quad (\text{S129})$$

$$W_{\text{II}} = V_3 - V_2, \quad (\text{S130})$$

$$W_{\text{IV}} = V_4 - V_5 + T_H \ln \frac{2V_4 - T_H}{2V_5 - T_H}, \quad (\text{S131})$$

$$W_{\text{V}} = V_1 - V_5, \quad (\text{S132})$$

and the operation time according to Eq. (S98) is

$$\tau_{\text{I}} = \frac{2(V_1 - V_2)}{\mathcal{H}}, \quad (\text{S133})$$

$$\tau_{\text{III}} = \frac{\kappa}{2\lambda_H} \ln \frac{2V_3 - T_H}{2V_4 - T_H}, \quad (\text{S134})$$

$$\tau_{\text{IV}} = \frac{2(V_4 - V_5)}{\mathcal{H}}. \quad (\text{S135})$$

The output power of the maximum- \mathcal{H} cycle according to Eq. (S40) is

$$P_{\text{over}} = - \frac{2V_1 - 2V_2 + V_3 + V_4 - 2V_5 + T_L \ln \frac{2V_1 - T_L}{2V_2 - T_L} + T_H \ln \frac{2V_4 - T_H}{2V_5 - T_H}}{\frac{8}{\lambda_L} \frac{(T_H + 3T_L)}{(T_H - T_L)^2} (V_1 - V_2 + V_4 - V_5) + \frac{1}{2\lambda_H} \ln \frac{2V_3 - T_H}{2V_4 - T_H}} \times \frac{1}{\kappa}. \quad (\text{S136})$$

We notice that the potential energies V_j of the maximum- \mathcal{H} cycle are solved previously by Eqs. (S108), (S111), and (S115)-(S118), and are independent of the friction coefficient κ . Therefore, we conclude the maximum output power (S136) in the overdamped limit is inversely proportional to κ .

To obtain the maximum power in the overdamped limit, we consider the sliced cycle constructed around the above two switchings. This follows from a simple argument that one can always divide a cycle into several slices, and some slice has the largest power among all slices. For the sliced cycles, the output power becomes equal to the pseudo-Hamiltonian. We will show this in Sec. IV. Therefore, the maximum power in the overdamped limit according to Eq. (S125) is

$$P_{\text{over}}^* = \frac{\lambda_H T_H}{\kappa} \phi\left(\frac{T_L}{T_H}\right) \approx \frac{(T_H - T_L)^2 \lambda_H}{4(3T_H + T_L)\kappa} \quad (\text{S137})$$

where $\phi(\theta)$ is given by Eq. (S126). We compare the precise and approximate results of the maximum power in Fig. S2.

IV. OUTPUT POWER OF SLICED CYCLE

A. Generic damped situation

We next consider the sliced cycles in generic damped situation. The diagram of a sliced cycle is shown in Fig. S3. Since the operation time of the two relaxation processes is short enough, we can neglect the change of stiffness during the two processes and just consider them as isochoric processes. Thus the cycle becomes an Otto cycle.

The potential energy of point 4 is related to that of point 3 as

$$V_4 = V_3 + dV_3. \quad (\text{S138})$$

According to the switchings, we obtain the potential energy at points 2 and 6 as

$$\frac{V_2}{\lambda_2} \sqrt{\kappa^2 + 2\lambda_2} = \frac{V_3}{\lambda_H} \sqrt{\kappa^2 + 2\lambda_H}, \quad (\text{S139})$$

$$\frac{V_6}{\lambda_2} \sqrt{\kappa^2 + 2\lambda_2} = \frac{V_4}{\lambda_H} \sqrt{\kappa^2 + 2\lambda_H}. \quad (\text{S140})$$

The work in the connecting processes is

$$W_{\text{II}} = (\sqrt{\kappa^2 + 2\lambda_H} - \sqrt{\kappa^2 + 2\lambda_2}) \frac{V_3}{\lambda_H} \sqrt{\kappa^2 + 2\lambda_H}, \quad (\text{S141})$$

$$W_{\text{V}} = (\sqrt{\kappa^2 + 2\lambda_2} - \sqrt{\kappa^2 + 2\lambda_H}) \frac{V_4}{\lambda_H} \sqrt{\kappa^2 + 2\lambda_H}. \quad (\text{S142})$$

The operation time of the isochoric processes is

$$\begin{aligned} \tau_{\text{III}} &= \frac{\kappa^2 + 2\lambda_H}{2\kappa\lambda_H} \ln \frac{T_H - 2V_3}{T_H - 2V_4} \\ &= \frac{\kappa^2 + 2\lambda_H}{\kappa\lambda_H} \frac{dV_3}{T_H - 2V_3}, \end{aligned} \quad (\text{S143})$$

and

$$\begin{aligned} \tau_{\text{VI}} &= \frac{\kappa^2 + 2\lambda_2}{2\kappa\lambda_2} \ln \frac{2V_6 - T_L}{2V_2 - T_L} \\ &= \frac{\kappa^2 + 2\lambda_2}{\kappa\lambda_2} \frac{dV_2}{2V_2 - T_L}. \end{aligned} \quad (\text{S144})$$

The output power is

$$\begin{aligned} P^{\text{slice}} &= -\frac{W_{\text{II}} + W_{\text{V}}}{\tau_{\text{III}} + \tau_{\text{VI}}} \\ &= \sqrt{\lambda_H} T_H \frac{\frac{\kappa}{\sqrt{\lambda_H}} (1 - \sqrt{\frac{\kappa^2 + 2\lambda_2}{\kappa^2 + 2\lambda_H}})}{\frac{T_H}{T_H - 2V_3} + \frac{\kappa^2 + 2\lambda_2}{\kappa^2 + 2\lambda_H} \frac{T_H}{2V_3 \frac{\lambda_2}{\lambda_H} - T_L \sqrt{\frac{\kappa^2 + 2\lambda_2}{\kappa^2 + 2\lambda_H}}}}. \end{aligned} \quad (\text{S145})$$

Let us define some dimensionless quantities

$$u = \frac{\kappa}{\sqrt{\lambda_H}}, \quad (\text{S146})$$

$$y = \frac{\lambda_2}{\lambda_H}, \quad (\text{S147})$$

$$z = \frac{2V_3}{T_H}, \quad (\text{S148})$$

$$v = \sqrt{\frac{u^2 + 2y}{u^2 + 2}}. \quad (\text{S149})$$

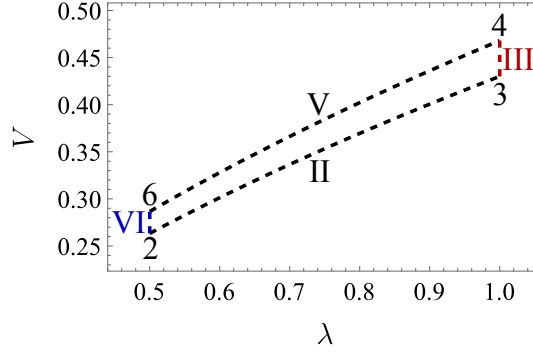


Figure S3. Diagram of a sliced cycle. It is an Otto cycle consisting of two adiabatic processes and two isochoric relaxation processes.

Then we rewrite the output power as

$$P^{\text{slice}} = \sqrt{\lambda_H T_H} h(z, v, y), \quad (\text{S150})$$

where we have defined a function

$$h(z, v, y) \equiv \frac{(1-v)}{\frac{1}{1-z} + \frac{v^2}{zy-\theta v}} \sqrt{\frac{2(v^2-y)}{1-v^2}}. \quad (\text{S151})$$

We optimize the function $h(z, v, y)$ under the constraints $v\theta/z < y < v^2 < 1$, $0 < z < 1$ to obtain a bound on the output power. We first choose the optimal

$$z^* = \frac{v(\theta + \sqrt{y})}{v\sqrt{y} + y}, \quad (\text{S152})$$

and we obtain

$$h(z^*, v, y) = \frac{\sqrt{2}(1-v)(y-\theta v)}{(v + \sqrt{y})^2} \sqrt{\frac{v^2-y}{1-v^2}}. \quad (\text{S153})$$

We further optimize v and y to obtain the global upper bound $h(z, v, y) \leq h(z^*, v^*, y^*) \equiv h_{\text{bound}}$, which can be represented as the positive root x of the following polynomial

$$\begin{aligned} & 729(\theta + 1)^2 x^{12} - 108(\theta^4 + 690\theta^3 + 7893\theta^2 + 12888\theta + 5940) x^{10} \\ & + 4(\theta^6 + 2610\theta^5 + 574425\theta^4 - 3453408\theta^3 - 148824\theta^2 - 2259360\theta - 1219536) x^8 \\ & - 128(3\theta^7 + 2131\theta^6 + 85745\theta^5 - 385087\theta^4 + 983572\theta^3 - 81252\theta^2 + 48816\theta + 11880) x^6 \\ & + 512(19\theta^8 + 1288\theta^7 + 31966\theta^6 - 82560\theta^5 - 157805\theta^4 - 46328\theta^3 + 11892\theta^2 - 16\theta + 8) x^4 \\ & - 8192\theta^2(3\theta^7 + 39\theta^6 + 1294\theta^5 + 3180\theta^4 + 2883\theta^3 + 811\theta^2 - 20\theta + 2) x^2 + 16384(\theta - 1)^4 \theta^4 (\theta + 1)^2 = 0, \end{aligned} \quad (\text{S154})$$

where v^* and y^* are solved from

$$-2\theta v^2 + v\sqrt{y}(\theta - 2v) + 2vy + y^{3/2} = 0, \quad (\text{S155})$$

$$\theta v^3 - 2(v^2 - 1)y^{3/2} + 2\theta v(v^2 - 1)\sqrt{y} + y(\theta + v^3 - (\theta + 1)v^2 - (\theta + 1)v) + y^2 = 0. \quad (\text{S156})$$

The bound on the output power is expressed by

$$P_{\text{bound}} = \sqrt{\lambda_H T_H} h_{\text{bound}}. \quad (\text{S157})$$

We can also maximize the power with given κ , namely, with given u maximizing

$$h(z^*, \sqrt{\frac{u^2 + 2y}{u^2 + 2}}, y) = \frac{u(1 - \sqrt{\frac{u^2 + 2y}{u^2 + 2}})(y - \theta\sqrt{\frac{u^2 + 2y}{u^2 + 2}})}{\left(\sqrt{\frac{u^2 + 2y}{u^2 + 2}} + \sqrt{y}\right)^2}. \quad (\text{S158})$$

The optimal choose of $y^*(u)$ with given u is the root of

$$2\theta^2 u^2 + y^{3/2}(\theta^2 + 4\theta - 2\theta u^2 - 2u^2) + y^2(-2\theta - 2u^2) + y(3\theta^2 - 2\theta u^2 + 2u^2) + 4\theta u^2 \sqrt{y} + (-2\theta - 4)y^{5/2} + y^{7/2} - y^3 = 0. \quad (\text{S159})$$

We denote the maximum value as

$$h^* \equiv h(z^*, \sqrt{\frac{u^2 + 2y}{u^2 + 2}}, y^*(u)). \quad (\text{S160})$$

We use the above results Eqs. (S154) and (S160) to plot the horizontal gray line and the black dotted curve in Fig. 3 of the main text.

B. Overdamped limit

In the overdamped limit $\kappa^2 \gg \lambda$ or $u \gg 1$, the power Eq. (S145) becomes

$$P_{\text{over}}^{\text{slice}} = \sqrt{\lambda_H} T_H h_{\text{over}}(z, y, u), \quad (\text{S161})$$

where the function $h_{\text{over}}(z, y, u)$ according to Eq. (S151) is

$$h_{\text{over}}(z, y, u) = \frac{1 - y}{\frac{1}{1 - z} + \frac{1}{zy - \theta}} \frac{1}{u}. \quad (\text{S162})$$

We have used the fact that $1 - v \approx (1 - y)/u^2$. For $0 < y < 1$ and $\theta/y < z < 1$, the maximum of h_{over} is exactly given by $\phi(\theta)/u$ solved from Eq. (S125).

C. Underdamped limit

In the underdamped limit $\kappa^2 \ll \lambda$ or $u \gg 1$, the power Eq. (S145) becomes

$$P_{\text{under}}^{\text{slice}} = \sqrt{\lambda_H} T_H h_{\text{under}}(z, y, u), \quad (\text{S163})$$

where the function $h_{\text{under}}(z, y, u)$ according to Eq. (S151) is

$$h_{\text{under}}(z, y, u) = \frac{(1 - \sqrt{y})(1 - z)(\sqrt{y}z - \theta)}{\sqrt{y} - \theta} u. \quad (\text{S164})$$

We have used the fact that $v \approx y$. For $\theta^2 < y < 1$ and $\theta/\sqrt{y} < z < 1$, the maximum of h_{under} is

$$h_{\text{under}}^* = \frac{1}{4} u (1 - \sqrt{\theta})^2, \quad (\text{S165})$$

which is reached by $y = \theta$ and $z = (1 + \sqrt{\theta})/2$. The output power then coincides with Eq. (S75).

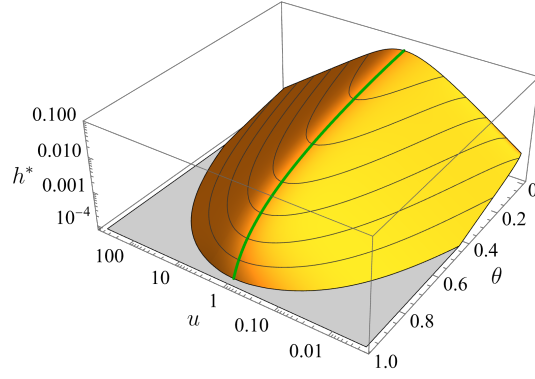


Figure S4. The maximum output power $P^* = \sqrt{\lambda_H T_H} h^*$ as a function of the friction coefficient u and the temperature ratio θ . The green solid curve shows the optimal choice of the friction coefficient to maximize the output power $P_{\text{bound}} = \sqrt{\lambda_H T_H} h_{\text{bound}}$. Here we choose $\lambda_H = 1$ and $T_H = 1$.

D. Maximum output power in generic damped situation

We show the maximum output power $P^* = \sqrt{\lambda_H T_H} h^*$ as a function of the friction coefficient u and the temperature ratio θ in Fig. S4. For given θ , large output power can be obtained by choosing an appropriate friction ratio reflecting by u . The bound of the output power $P_{\text{bound}} = \sqrt{\lambda_H T_H} h_{\text{bound}}$ is shown by the green solid curve. Here we choose $\lambda_H = 1$ and $T_H = 1$. The definitions of h_{bound} and h^* are given by Eqs. (S154) and (S160), respectively.

-
- [S1] L. S. Pontryagin, V. G. Boltyanskii, R. V. Gamkrelidze, and E. F. Mishechenko, *The Mathematical Theory of Optimal Processes* (Wiley, New York, 1962).
[S2] Z. Gong, Y. Lan, and H. Quan, *Phys. Rev. Lett.* **117**, 180603 (2016).
[S3] A. Dechant, N. Kiesel, and E. Lutz, *Europhys. Lett.* **119**, 50003 (2017).
[S4] D. S. P. Salazar, *Phys. Rev. E* **101**, 030101(R) (2020).
[S5] Y. H. Chen, J.-F. Chen, Z. Fei, and H. T. Quan, *Phys. Rev. E* **106**, 024105 (2022).
[S6] T. Schmiedl and U. Seifert, *Phys. Rev. Lett.* **98**, 108301 (2007).
[S7] T. Schmiedl and U. Seifert, *Europhys. Lett.* **81**, 20003 (2007).